Journal of Advanced Ceramics
2015, **4**(2): 123–129
DOI: 10.1007/s40145-015-0142-4

ISSN 2226-4108
CN 10-1154/TQ

Research Article

Annealing effects on the structural and optical properties of ZnO nanoparticles with PVA and CA as chelating agents

A. N. MALLIKA*, A. Ramachandra REDDY, K. Venugopal REDDY

Department of Physics, *Materials Science Laboratory*, *National Institute of Technology*, *Warangal-506004*, *Telangana*, *India*

Received: November 14, 2014; Revised: December 30, 2014; Accepted: January 24, 2015

Abstract: The effects of annealing temperatures and chelating agents on the structural and optical properties of ZnO nanoparticles were investigated. The average particle size of ZnO nanoparticles increased with increase of annealing temperatures. The decrease of the full width at half maximum (FWHM) with increasing annealing temperatures inferred increase of particle/grain growth. The grain sizes were also observed to be increased with increase of annealing temperatures. From the absorption spectra of the samples, the absorption was red-shifted and the energy band gap was blue-shifted with increase of annealing temperatures. A sharp UV emission peak was observed and the intensity of this peak increased with annealing temperatures corresponding to the high crystallinity in the samples. At high annealing temperature of 700 ℃, ZnO exhibited a less intense deep level emission. This negligible deep level emission was attributed to the oxygen vacancies created at higher annealing temperatures.

Keywords: ZnO nanostructures; citric acid (CA); polyvinyl alcohol (PVA); chelating agents; scanning electron microscopy (SEM); optical properties

1 Introduction

Zinc oxide (ZnO) is a wide-band-gap, wurtzite-type semiconductor with an energy gap of 3.37 eV at room temperature. The large exciton binding energy and the wide band gap make it an excellent semiconductor material for applications considered for other wide-band-gap materials such as GaN and SiC. Nanomaterials and nanostructures have shown their great potential in basic scientific research and technology applications due to their size effect and their promising applications in nano scaled devices [1]. As a versatile semiconductor, ZnO is a potential functional material exhibiting many technological applications in photonic crystals, photo detectors, varistors, solar cells, transparent conductive films, and bulk acoustic wave devices and so on [2,3]. Furthermore, its properties can be tailored by synthesizing particles of specific size, especially in nano size. The ZnO nanocrystals always exhibit novel unique properties due to quantum confinement effects compared with the bulk ZnO [4]. Nevertheless, the properties of the ZnO nanocrystals depend closely on their particle size, morphology, surface area, and activity [5]. Further, to monitor the material properties in a controllable fashion, suitable temperatures and annealing ambient environment have to be chosen [6]. Numerous studies have reported that an optimum annealing treatment not only improves the crystallinity

* Corresponding author.
E-mail: mallika.nitw@gmail.com

of ZnO, but also changes the Zn/O ratio and intrinsic defects [7]. Singh *et al*. [8] have reported the thermal annealing effects on the structural and optical properties of ZnO in terms of coarsening mechanism. With modified sol–gel combustion method, Zak *et al*. [9] have studied the structural and optical properties. At 500 ℃ annealing temperature, Yang *et al*. [10] have observed good emission properties with fewer defects. Kazemi *et al*. [11] have investigated the significant role of complexing agents on the structural and optical properties of ZnO nanoparticles with annealing treatment. However, the systematic study of the influence of annealing treatment on the structural and optical properties of ZnO nanoparticles with citric acid and polyvinyl alcohol as chelating agents has few reports.

In the present study, ZnO nanoparticles were prepared with citric acid (CA) and polyvinyl alcohol (PVA) as chelating agents. The samples were annealed at temperatures 400 ℃, 500 ℃, 600 ℃, and 700 ℃. The structural properties of the prepared samples were investigated by X-ray diffraction (XRD) and scanning electron microscopy (SEM). The optical properties were studied with Fourier transform infrared spectroscopy (FTIR), absorption spectroscopy, and photoluminescence (PL) emission spectra. Based on the results, the effect of annealing treatment with chelating agents on the structural and optical properties was discussed.

2 Experimental

For preparing ZnO nanoparticles, $Zn(NO_3)_2{\cdot}6H_2O$, $C_6H_8O_7$, and $[–CH_2CHOH–]_n$ were taken as the starting chemicals. Zinc nitrate to chelating agent ratio was maintained as 1:3 throughout the experiment. In order to get 2 g of the final product, 0.8 M zinc nitrate was first dissolved in 30 mL of deionised water. Then, 6 g of polyvinyl alcohol (PVA) was dissolved slowly in 60 mL of deionised water, and stirred vigorously till a homogenous milk white solution was obtained. Then, zinc nitrate solution was added dropwise to chelating (PVA) solution. This milk white solution was vigorously stirred on hot plate at 70 ℃ till the gel formation. The gel was kept in an oven to get dried powders at 100 ℃ for 6 h. Finally, the as-prepared powders were annealed in a programmable muffle furnace with annealing rate 2 ℃/min to different annealing temperatures 400 ℃, 500 ℃, 600 ℃, and 700 ℃ and holding time 1 h. The same procedure was followed to prepare ZnO nanoparticles with citric acid (CA) as chelating agent. The samples were coded as per the annealing temperatures for simple understanding. For temperatures 400 ℃, 500 ℃, 600 ℃, and 700 ℃, the samples were coded as CA400, CA500, CA600, and CA700 with CA as chelating agent, respectively. In the same manner, PVA samples were also coded as PVA400, PVA500, PVA600, and PVA700 for temperatures 400 ℃, 500 ℃, 600 ℃, and 700 ℃, respectively.

The phase identification and crystallite sizes of the samples were determined using XRD patterns recorded on INEL XRG 3000 powder diffractometer equipped with Co Kα radiation ($\lambda = 1.7889$ Å) in terms of 2θ ranging from 20° to 120°. The morphology of the samples was studied with SEM model VEGA3TESCAN along with energy dispersive spectrometer (EDS). Formation of ZnO was confirmed from FTIR spectrum (Model: Perkin Elmer Spectrum-100) recorded in the wavenumber region 4000–400 cm^{-1}. Optical absorption of the samples was recorded using UV–visible (UV–Vis) spectrophotometer (Model: Varian, Cary 5000) in the wavelength region 250–600 nm. The PL measurements were performed on Jobin yuon spectrofluorometer (Model: Fluorolog-Fl3-11) equipped with a xenon lamp of 450 W.

3 Results and discussion

3.1 X-ray diffraction

The XRD patterns of ZnO nanoparticles prepared with CA and PVA as chelating agents at annealing treatments 400 ℃, 500 ℃, 600 ℃, and 700 ℃ are given in Fig. 1. The reflection peaks at $2\theta = 37.123°$, 40.246°, 42.284°, 55.850°, 67.029°, and 74.369° correspond to (100), (002), (101), (102), (110), and (103) reflection planes of ZnO hexagonal wurtzite structure, respectively. The XRD spectra reveal the influence of annealing treatments on the structural properties. The intensity of the peaks gets sharpened and increased with increasing annealing temperatures for both CA and PVA samples. Primarily, the increase in the peak intensities is attributed to increase of the crystallinity and crystallite size. In general, for ZnO there are many dangling bonds related to the zinc and oxygen defects at the grain boundaries. As a result, these defects are favourable for the merging process to form larger ZnO grain when increasing the annealing

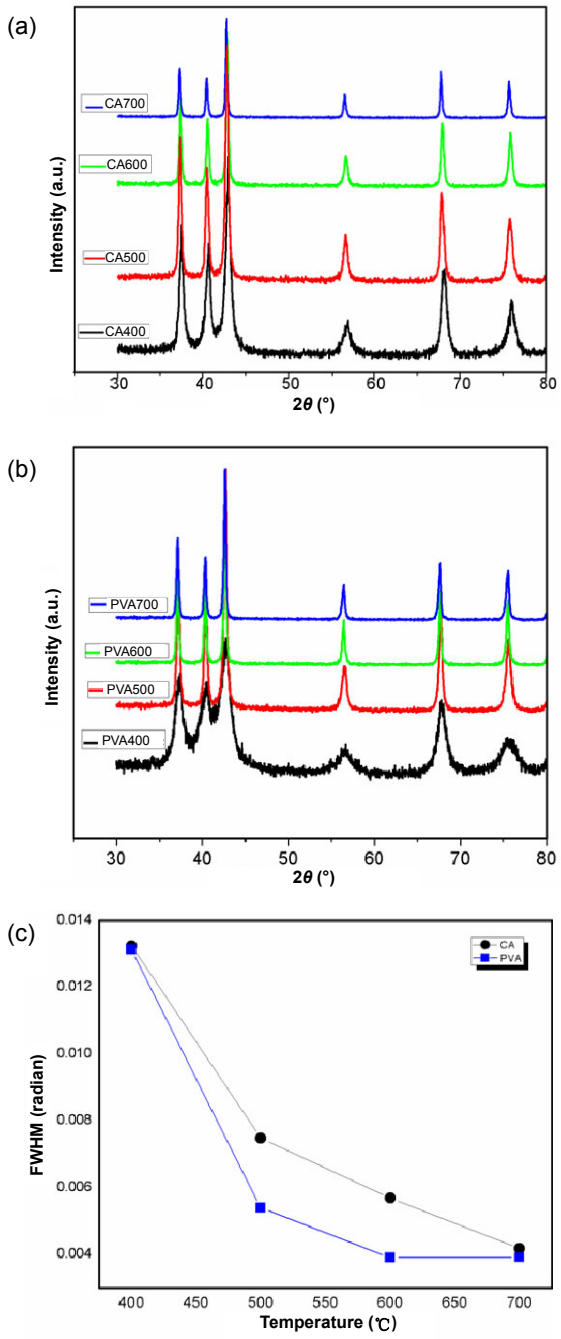

Fig. 1 (a) and (b) XRD patterns of ZnO nanoparticles annealed at temperatures 400 ℃, 500 ℃, 600 ℃, and 700 ℃ with (a) CA and (b) PVA as chelating agents. (c) Variation of the FWHM with annealing treatments.

temperatures [12]. The average crystallite sizes of all the samples were calculated using Debye–Scherrer formula [13] and are tabulated in Table 1. The average crystallite sizes increase with increasing annealing temperatures, from 13 (at 400 ℃) to 41 nm (at 700 ℃) for CA samples. For PVA samples, it has increased from 7 (at 400 ℃) to 36 nm (at 700 ℃). In addition,

Table 1 Crystallite size *D* estimated from the FWHM values at different annealing temperatures

Temperature (℃)	CA as chelating agent		PVA as chelating agent	
	FWHM (radian)	*D* (nm)	FWHM (radian)	*D* (nm)
400	0.01324	13	0.023230	7
500	0.00749	23	0.007400	23
600	0.00570	30	0.004680	35
700	0.00418	41	0.004704	36

the full width at half maximum (FWHM) values decrease with increase of annealing temperatures as shown in Fig. 1(c). The changes in FWHM can be correlated to the grain sizes [14]; the smaller FWHM indicates a larger grain size and a better crystal quality, which may be due to the recrystallization process with sufficient thermal energy supply.

3. 2 Scanning electron microscopy

Microstructural characterization of synthesized samples was studied by SEM analysis. For morphological studies, gold coating was provided on the powder sample placed over a carbon tape. Figures 2(a) and 2(b) depict the SEM images of ZnO nanostructure with CA and PVA as chelating agents annealed at various temperatures, respectively. The grain size of the samples was determined by counting sufficiently large number of grains to ensure the accuracy. The average grain size of PVA and CA samples is in the range of 50–100 nm as indicated in Figs. 2(a) and 2(b). With increasing annealing temperatures, the grain growth is observed in both samples. The compositions of ZnO nanoparticles with different chelating agents were determined through EDS, which is shown in Fig. 2(c).

3. 3 Fourier transform infrared spectroscopy

Chemical and structural changes that take place during the heat treatment can be monitored by a spectroscopic analysis. Figure 3 depicts the FTIR spectra of the annealed samples CA400, CA500, CA600, CA700, PVA400, PVA500, PVA600, and PVA700. Two strong frequency bands are observed in all the samples at 556–445 cm^{-1} corresponding to characteristics of ZnO wurtzite structure [15]. The peaks observed at 1600 and 1384 cm^{-1} are assigned to the asymmetrical and symmetrical stretching of zinc carboxylate, respectively [16]. Further, for PVA samples these peaks persist till higher annealing temperatures, whereas for CA they are eliminated completely. This may be analysed as following: as the size of the nanoparticles

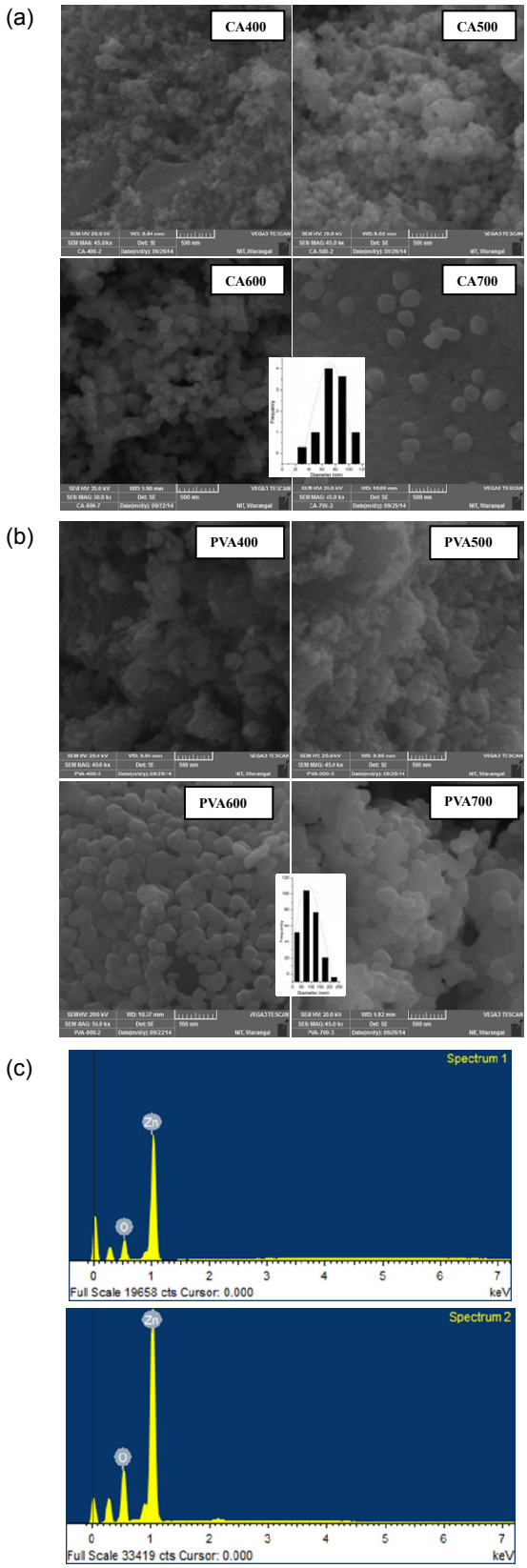

Fig. 2 (a) and (b) Morphology of ZnO nanoparticles annealed at temperatures 400 ℃, 500 ℃, 600 ℃, and 700 ℃ with (a) CA and (b) PVA as chelating agents. (c) Compositions of ZnO nanoparticles with CA (upper) and PVA (lower) as chelating agents.

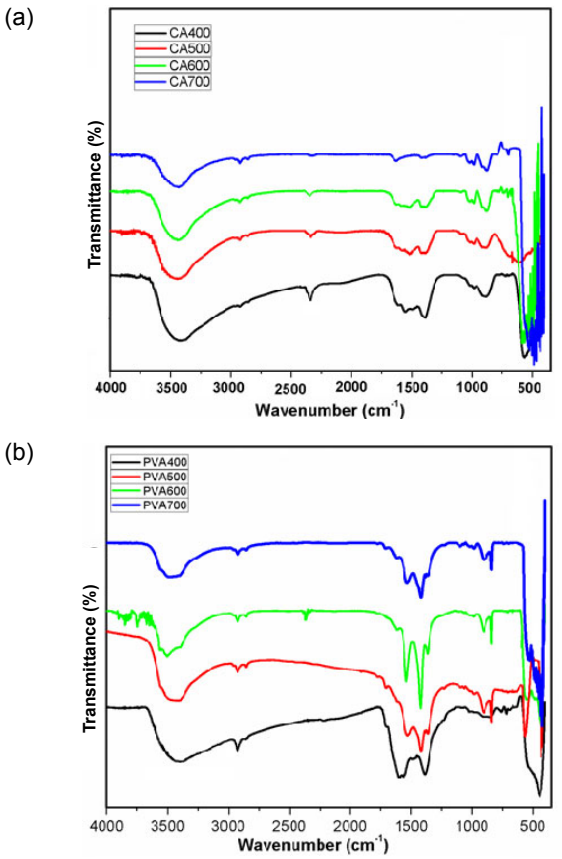

Fig. 3 FTIR spectra of ZnO with (a) CA and (b) PVA as chelating agents.

increases with increase of annealing temperatures, the content of the carboxylate (COO–) and hydroxyl (–OH) groups in the samples decreases. The carboxylate probably comes from reactive carbon containing plasma species during synthesis and the hydroxyl results from the hygroscopic nature of ZnO. Annealing at 700 ℃ significantly reduces these carboxylate and hydroxyl impurities in all samples for CA, whereas for PVA they persist till higher temperatures as shown in Fig. 3. Besides this, a band around 1384 cm^{-1} is attributed to the anti-symmetric NO_3^{-1} stretching vibration [17]. In addition to these bands, there is a low-intensity frequency band around 2900 cm^{-1} corresponding to the stretching vibration of CH_2 implying the presence of PVA and CA [18]. It has been confirmed from these bands that small amount of the chelating agent present on the surface of the sample which stabilizes the ZnO nanostructures [19]. The intensity of these bands reduces as a function of annealing temperature indicating the formation of pure wurtzite structure. Together, this suggests that these FTIR-identified impurities mainly exist near ZnO surface.

3. 4 UV-Vis absorption

The UV–Vis absorption spectra of the ZnO nanoparticles prepared with CA and PVA as chelating agents annealed at temperatures 400 ℃, 500 ℃, 600 ℃, and 700 ℃ are shown in Fig. 4(a). The relevant increase in the absorption at wavelengths less than 400 nm can be assigned to the intrinsic band-gap absorption of ZnO due to the electron transitions from the valence band to the conduction band (O_{2p}–Zn_{3d}) [20]. Interestingly, an obvious red shift in the absorption edge is observed for both the products. Zak *et al*. [9] have observed the same phenomenon; this may be assigned to changes in their morphologies, particle size, and surface microstructures. A practical method is to equate E_g with the wavelength at which the absorption is 50% of the excitonic peak (shoulder), called $\lambda_{1/2}$ [21]. This is schematically shown in Fig. 4(b). The energy band gap $E_g(\lambda_{1/2})$ of ZnO nanoparticles calculated are shown in Table 2. The increase in the ZnO band gap energy is in good agreement with the corresponding red shift observed in the absorption edge mentioned above. Further, from effective mass approximation, the energy corresponding to the exciton absorption peak has been converted in terms of particle size [22]:

$$E = E_g + h^2\pi^2\left(\frac{1}{m_e} + \frac{1}{m_h}\right) - \left(\frac{1.8e^2}{4\pi\varepsilon'\varepsilon_0 R}\right) + \text{smaller term}$$

where E is the band gap of the synthesised particle; E_g is the bulk energy of ZnO; R is the radius of the particle; m_e is the effective mass of the electron ($0.28m_0$); m_h is the effective mass of the hole ($0.49m_0$); ε' is the dielectric constant of the material (9.1); ε_0 is the permittivity of the free space; and h is the Planck's constant. The obtained values of the particle radius using the mass approximation are observed to be increased with increase of the annealing temperatures and are tabulated in Table 2.

Table 2 Particle size *R* value using effective mass approximation and their corresponding energy band gap value with varying annealing temperatures

Temperature (℃)	Energy band gap (eV)		Particle size *R* (nm)	
	CA as chelating agent	PVA as chelating agent	CA as chelating agent	PVA as chelating agent
400	3.14	2.99	2.37	2.44
500	3.17	3.16	2.79	2.62
600	3.19	3.19	2.92	3.24
700	3.20	3.20	2.85	2.79

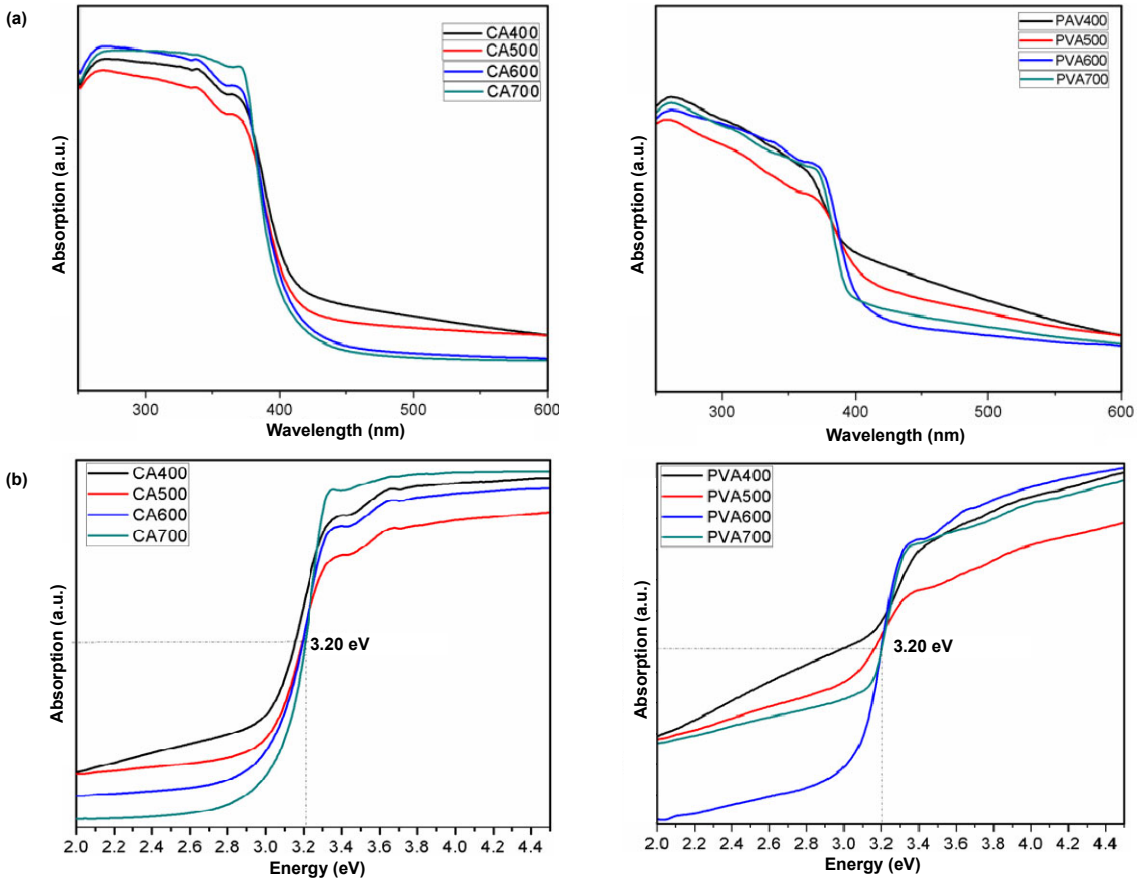

Fig. 4 (a) Absorption of ZnO nanoparticles annealed at different temperatures; (b) absorption profile of ZnO with annealing treatments

3. 5 Photoluminescence

The PL spectroscopy is an effective method to investigate the presence of defects in semiconductors [23]. Figure 5 shows the PL spectra of ZnO nanoparticles annealed at different temperatures with CA and PVA as chelating agents. It is observed from the Fig. 5 that, ZnO nanoparticles exhibit a strong excitonic related UV emission positioned at 395 nm for all the annealing temperatures. The intensity of this UV emission peak increases monotonously with increase of annealing temperatures. As the increase in the UV emission is associated with the grain and crystal orientation [24], this can be further analysed as, with increase of the annealing temperatures, there is a reduction in the grain boundaries and the number of particles on the surface of ZnO nanoparticles. Consequently, the number of non-radiative transitions and deep level defects are supressed together, and thereby UV emission intensity has increased [6]. This can be further attributed to the reduciton of the carboxylates and hydroxyl impurities with increase of annelaing temperatures as observed in FTIR analysis. As the carboxylates and hydroxyl impurites serve as the non-radiative recombination centers during the relaxation process, the non-radiative transitions are supressed. This behaviour indicates the improvement in the crystalline nature of the samples [25]. With increasing annelaing temperatures, some defect related emission is observed at higher temperature (700 ℃). In general, for the high-temperature annealing in air, the formation of Zn_i (zinc interstitials) and V_O (oxygen vacancies) is favourable [26]. Therefore, in the present study, the negligible emission occurring at high temperature 700 ℃ may be assigned to Zn_i and V_O defect states.

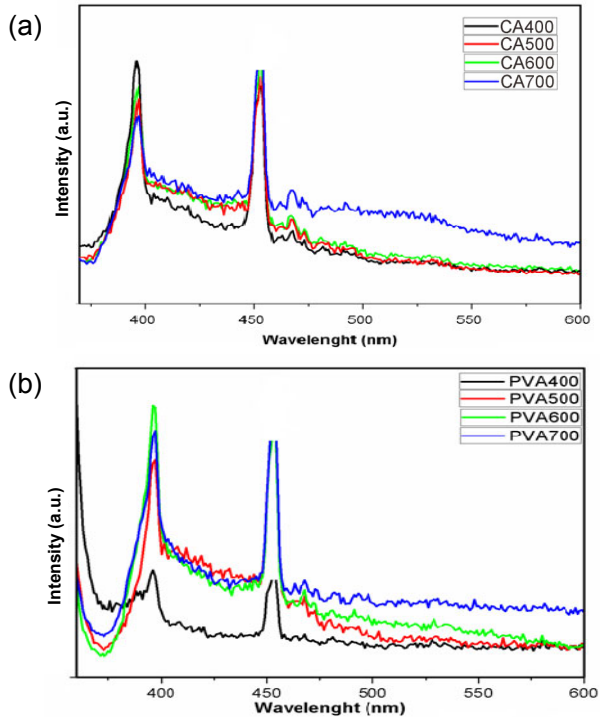

Fig. 5 PL spectra of ZnO annealed at temperatures 400 ℃, 500 ℃, 600 ℃, and 700 ℃ with (a) CA and (b) PVA as chelating agents.

4 Conclusions

The wurtzite structure of ZnO was confirmed from the diffraction patterns of the samples. The average particle sizes estimated from the XRD results were observed to be increased with increasing annealing temperatures for both CA and PVA samples. The reduction in the FWHM with increasing temperatures has confirmed the improved crystallinity of the samples. The grain growth was further confirmed from SEM. From FTIR studies, with increase of annealing temperatures, the presence of carboxylate and hydroxyl impurities was reduced as the particle size increased. Further, this was reflected in the emission spectra, as the non-radiative recombination transitions were suppressed with increase of the particle sizes with increase of annealing temperatures. The optical band gap of the samples was blue-shifted with temperatures indicating particle size growth, and the particle sizes estimated using effective mass approximation corroborated the same. The increase in the intensity of the UV emission peaks with increase of annealing temperatures corroborated the XRD results. Along with a strong UV emission, some defect related emissions exhibited at higher temperature 700 ℃. This defect related emission was assigned to the oxygen vacancies created at higher annealing temperatures.

Acknowledgements

The authors are thankful to the dean of School of Physics, University of Hyderabad, for providing XRD facility. The authors also would like to thank the Sophisticated Analytical Instrument Facility (SAIF) STIC India, Cochin, for the characterization of absorption spectra of the samples.

References

[1] Uthirakumar P, Hong C-H. Effect of annealing temperature and pH on morphology and optical property of highly dispersible ZnO nanoparticles. *Mater Charact* 2009, **60**: 1305–1310.

[2] Lee JB, Kim HJ, Kim SG, *et al*. Deposition of ZnO thin films by magnetron sputtering for a film bulk acoustic resonator. *Thin Solid Films* 2003, **435**: 179–185.

[3] Minami T, Ida S, Miyata T, *et al*. Transparent conducting ZnO thin films deposited by vacuum arc plasma evaporation. *Thin Solid Films* 2003, **445**: 268–273.

[4] Seelig EW, Tang B, Yamilov A, *et al*. Self-assembled 3D photonic crystals from ZnO colloidal spheres. *Mater Chem Phys* 2003, **80**: 257–263.

[5] Hu Y, Chen H-J. Preparation and characterization of nanocrystalline ZnO particles from a hydrothermal process. *J Nanopart Res* 2008, **10**: 401–407.

[6] Dutta S, Chattopadhyay S, Sarkar A, *et al*. Role of defects in tailoring structural, electrical and optical properties of ZnO. *Prog Mater Sci* 2009, **54**: 89–136

[7] Fang ZB, Yan ZJ, Tan YS, *et al*. Influence of post-annealing treatment on the structure properties of ZnO films. *Appl Surf Sci* 2005, **241**: 303–308.

[8] Singh RG, Singh F, Kumar V, *et al*. Growth kinetics of ZnO nanocrystallites: Structural, optical and photoluminescence properties tuned by thermal annealing. *Curr Appl Phys* 2011, **11**: 624–630.

[9] Zak AK, Abrishami ME, Abd MWH, *et al*. Effects of annealing temperature on some structural and optical properties of ZnO nanoparticles prepared by a modified sol–gel combustion method. *Ceram Int* 2011, **37**: 393–398.

[10] Yang J, Liu X, Wang Y, *et al*. Effect of annealing temperature on the structure and optical properties of ZnO nanoparticles. *J Alloys Compd* 2009, **477**: 632–635.

[11] Kazemi A, Abadyan M, Ketabi A. Controlled structural and optical properties of ZnO nano-particles. *Phys Scr* 2010, **82**: 035801.

[12] Kuo S-Y, Chen W-C, Cheng C-P. Investigation of annealing-treatment on the optical and electrical properties of sol–gel-derived zinc oxide thin films. *Superlattice Microst* 2006, **39**: 162–170.

[13] Mallika AN, Reddy AR, Babu KS, *et al*. Synthesis and optical characterization of aluminum doped ZnO nanoparticles. *Ceram Int* 2014, **40**: 12171–12177.

[14] Ravichandran C, Srinivasan G, Lennon C, *et al*. Influence of post-deposition annealing on the structural, optical and electrical properties of Li and Mg co-doped ZnO thin films deposited by sol–gel technique. *Superlattice Microst* 2011, **49**: 527–536.

[15] Mallika AN, Reddy AR, Babu KS, *et al*. Structural and photoluminescence properties of Mg substituted ZnO nanoparticles. *Opt Mater* 2014, **36**: 879–884.

[16] Xiong G, Pal U, Serrano JG, *et al*. Photoluminescence and FTIR study of ZnO nanoparticles: The impurity and defect perspective. *Phys Status Solidi c* 2006, **3**: 3577–3581.

[17] Sujatha Ch., Reddy KV, Babu KS, *et al*. Effects of heat treatment conditions on the structural and magnetic properties of MgCuZn nano ferrite. *Ceram Int* 2012, **38**: 5813–5820.

[18] Kim SJ, Park SJ, Kim SI. Swelling behavior of interpenetrating polymer network hydro gels composed of poly(vinyl alcohol) and chitosan. *Reactive & Functional Polymers* 2003, **55**: 53–59.

[19] Razavi RS, Loghman-Estarki MR, Farhadi-Khouzani M, *et al*. Large scale synthesis of zinc oxide nano- and submicro-structures by Pechinis method: Effect of ethylene glycol/citric acid mole ratio on structural and optical properties. *Curr Nanosci* 2011, **7**: 807–812.

[20] Yu H, Yu J, Cheng B, *et al*. Effects of hydrothermal post-treatment on microstructures and morphology of titanate nanoribbons. *J Solid State Chem* 2006, **179**: 349–354.

[21] Sharma A, Singh BP, Dhar S, *et al*. Effect of surface groups on the luminescence property of ZnO nanoparticles synthesized by sol–gel route. *Surf Sci* 2012, **606**: L13–L17.

[22] Singh AK, Viswanath V, Janu VC. Synthesis, effect of capping agents, structural, optical and photoluminescence properties of ZnO nanoparticles. *J Lumin* 2009, **129**: 874–878.

[23] Srinet G, Varshney P, Kumar R, *et al*. Structural, optical and magnetic properties of $Zn_{1-x}Co_xO$ prepared by the sol–gel route. *Ceram Int* 2013, **39**: 6077–6085.

[24] Hsieh PT, Chen YC, Kao KS, *et al*. The ultraviolet emission mechanism of ZnO thin film fabricated by sol–gel technology. *J Eur Ceram Soc* 2007, **27**: 3815–3818.

[25] Gondal MA, Drmosh QA, Yamani ZH, *et al*. Synthesis of ZnO_2 nanoparticles by laser ablation in liquid and their annealing transformation into ZnO nanoparticles. *Appl Surf Sci* 2009, **256**: 298–304.

[26] Xu J, Shi S, Zhang X, *et al*. Structural and optical properties of (Al,K)-co-doped ZnO thin films deposited by a sol–gel technique. *Mat Sci Semicon Proc* 2013, **16**: 732–737.